# Temperature Dependent Short-Term Evaluation of index and performance tests on Bituminous Geomembranes

Mitchell Rogal[1], I.R. Fleming[1], B. Marcotte[1] and S. Bhat[2]
[1]*Department of Civil Geological & Environmental Engineering – University of Saskatchewan, Saskatoon, Canada*
[2]*Titan Environmental Containment Ltd.*

ABSTRACT

At GeoNiagara 2021, results of basic modified puncture and tearing index testing of BGMs were presented regarding performance at different temperatures. This paper contains new data on those results at subzero temperatures, as well as large scale laboratory performance testing at the same temperature range including both warm and sub-zero temperatures, and comparing these results to that of high density polyethylene (HDPE) geomembranes. The performance tests were completed using custom loading frames and performance apparatus in heated climate chambers and commercial walk-in freezer units.

There are advantages to bituminous over polymeric GMs, chiefly, high strength, elongation, puncture resistance and high soil interface shear resistance. Underwater installation is made easier by the fact that BGMs are denser than water and most installations benefit from the limited tendency for wrinkling when exposed to thermal and solar radiation. However, the lack of public peer-reviewed data does add some uncertainty for designers considering using BGMs for barrier systems. The lack of peer reviewed studies heavily limits the use of BGMs. This paper presents updated results of modified index tests and new large-scale performance tests of BGM at warm and sub-zero temperatures. Overall, there were noticeable variations in puncture resistance/displacement required to puncture in all samples with temperature changes, and changes in the peak/ post peak reaction of the sample within the tear tests. The large-scale testing showed how the ductility of BGMs can provide substantial benefits over HDPE as well.

RÉSUMÉ

Lors de GeoNiagara 2021, les résultats des tests de base des indices de perforation et de déchirure modifiés des BGM ont été présentés en ce qui concerne les performances à différentes températures. Cet article contient de nouvelles données sur ces résultats à des températures inférieures à zéro, ainsi que des tests de performance en laboratoire à grande échelle dans la même plage de températures, y compris les températures chaudes et inférieures à zéro. Les tests de performance ont été effectués à l'aide de cadres de chargement personnalisés et d'appareils de performance dans des chambres de climat chauffées et des congélateurs-chambres commerciaux.

Il y a des avantages à bitumineux par rapport aux MG polymères, principalement, à haute résistance, à l'allongement, à la résistance à la perforation et à la résistance élevée au cisaillement de l'interface du sol. L'installation sous-marine est facilitée par le fait que les BGM sont plus denses que l'eau et que la plupart des installations bénéficient de la tendance limitée à froissement lorsqu'elles sont exposées au rayonnement thermique et solaire. Cependant, le manque de données publiques évaluées par des pairs ajoute une certaine incertitude pour les concepteurs qui envisagent d'utiliser des BGM pour les systèmes barrières. L'absence d'études évaluées par des pairs limite fortement l'utilisation des BGM. Cet article présente les résultats mis à jour des tests d'indice modifiés et des nouveaux tests de performance à grande échelle de la BGM à des températures chaudes et inférieures à zéro. Dans l'ensemble, il y avait des variations notables dans la résistance à la perforation/le déplacement requis pour perforer dans tous les échantillons avec des changements de température, et des changements dans la réaction pic/post pic de l'échantillon dans les tests de déchirure. Les tests à grande échelle ont montré comment la ductilité des BGM peut également offrir des avantages substantiels par rapport au PEHD.

## INTRODUCTION

Geomembranes are a variety of non-porous media, meaning that there are no void spaces present within the material. However, fluid transport still occurs through the material at the molecular level via diffusion (Lambert et al. 2000). Driving forces of this diffusion include: concentration, temperature gradients, and hydraulic gradients (Touze-foltz et al. 2015). The bituminous aspect of BGMs is intended to act as an additional defense against some of these methods of diffusion.

One of the most common deterrents to using bituminous geomembranes in the lack of credible data on their performance in relation to their manufacturer specifications. Ongoing research into leakage and puncture of BGMs is taking place at Queen's University in Ontario by M. Clinton and K. Rowe (2017), however more needs to be conducted to increase their viability versus the existing geomembrane barrier products. One of the main aspects of this research is the comparison of the performance of BGMs at a wide range of temperatures. Saskatchewan's semi-arid climate is a perfect example of why this research can be beneficial, as the temperature can vary by over 60°C between seasons. This wide range of temperatures can greatly impact the initial performance of the BGM when it is installed and is an important aspect to consider in addition to loading performance and leakage resistance.

## 1 MATERIALS & METHODS

### 1.1 Selection of Bituminous Geomembranes

Two variations of the Coletanche elastic elastomeric BGMs were selected to be used in this testing, the ES2 and ES4 types, which were selected as they are two of the most popular BGM products that are offered. They are also close to the average specifications of the ES line of products in terms of properties Coletanche Inc. (2020).

Tables 1-2, and 3-4 contain technical specifications of the ES2 and ES4 products respectively, and were gathered from the Coletanche manufacturer technical sheets provided by Axter Coletanche Inc. 2009a/b.

#### 1.1.1 ES2 and ES4 Characteristics

The ES2 and ES4 are composed of 5 main components. The material compositions are shown in Table 1 and 3 respectively.

Table 1. Composition of ES2

| Material | Value (g/m$^2$) | Purpose |
|---|---|---|
| Glass Mat | 50 | Reinforcement |
| Non-woven Geotextile | 250 | Reinforcement |
| Elastomeric SBS | 4300 | Binder |
| Sand | 200 | Surface Finish |
| Polyester Anti-root film | 15 | Surface Finish |

Technical specifications of the Coletanche ES2 and ES4 BGMs can be seen below in Table 2 and 4 respectively.

Table 2. Technical Specs of ES2

| Characteristic | Value | Units |
|---|---|---|
| Thickness | 4.0 | mm |
| Surface Mass | 4.85 | kg/m$^2$ |
| Tearing Res. (MD/XD) | 825/700 | N |
| Max Tensile Str. (MD/XD)[1] | 27/24 | kN/m |
| Elongation (MD/XD)[1] | 60/60 | % |
| Static Puncture Res.[2] | 530 | N |

[1] As per ASTM D 7275
[2] As per ASTM D 4833

Table 3. Composition of ES4

| Material | Value (g/m$^2$) | Purpose |
|---|---|---|
| Glass Mat | 50 | Reinforcement |
| Non-woven Geotextile | 400 | Reinforcement |
| Elastomeric SBS | 5400 | Binder |
| Sand | 200 | Surface Finish |
| Polyester Anti-root film | 15 | Surface Finish |

Table 4. Technical Specs of ES4

| Characteristic | Value | Units |
|---|---|---|
| Thickness | 5.60 | mm |
| Surface Mass | 6.40 | kg/m$^2$ |
| Tearing Res. (MD/XD) | 1225/1025 | N |
| Max Tensile Str. (MD/XD)[1] | 39/31 | kN/m |
| Elongation (MD/XD)[1] | 60/60 | % |
| Static Puncture Res.[2] | 650 | N |

[1] As per ASTM D 7275
[2] As per ASTM D 4833

### 2.2 HDPE Geomembrane Selection

Two types of HDPE geomembranes were selected and compared to the results of the BGM testing. These products are the Solmax Smooth HDPE geomembranes at 1.5mm and 3mm thicknesses.

### 2.3 Testing Methods

The puncture method used in the initial stages of temperature varying testing was the ASTM D 4833, used for evaluating Geomembrane puncture resistance. The ASTM procedure was followed for both the ES2 and ES4 products, as well as the HDPE geomembrane.

The tearing tests follow the ASTM D 5884 test method used to determine the tearing strength of geomembranes. The practice for this ASTM test was followed for both the ES samples, as well as the HDPE samples.

A slight modification was implemented to both ASTM standards where tests were performed at different temperature increments of -20°C, -10°C, 0°C, 5°C, 10°C, 20°C, and 30°C.

## 2.4 Pneumatic Cylinder Frame

The frame used for testing is a custom 10 in. pneumatic cylinder frame with an operating pressure of roughly 250 psi which translates to around 87 kN of force.

The air flow is controlled using an electronic air regular which can be programmed to maintain, increase, and decrease the airflow applied to the system via a python script, and allows for multi-stage tests that run for days at a time, but still displays the applied airflow in PSI. Data logging is completed with a load cell attached to the top of the frame which is compressed/ put in tension depending on the tests. The data is sent to and compiled by a VLab software that can calibrate the data based on the defined specifications of the load cell itself. Although there are some disadvantages to using an air cylinder compared to hydraulic such as the potential of leakage, the mobility of the unit makes it easy to move in and out of the temperature controlled environments.

Figure 1: Pneumatic Cylinder frame with the controls present.

## 2.5 ASTM Puncture Assembly

The second piece of equipment used in this testing was a custom fabricated puncture apparatus specified by ASTM D 4833 (2010). The setup consists of two pieces: the probe which used for puncture, and the mounting frame used to hold the geomembrane sample (Rogal et al., 2021). The probe consists of a machined rod base, beveled into a 50mm long, 8mm diameter tip with a 0.8mm, 45° chamfer to the tip. The probe also has a threaded base to allow it to be connected to the load cell used in the tests (Rogal et al., 2021). Figure 2 shows the apparatus.

The base of the apparatus consists of a hollow cylindrical body welded to a base plate for stability. Attached to the top of the cylinder is a 4mm thick, 100mm diameter annulus with a 37mm diameter opening in the center. Equally spaced around the disc on a 45mm diameter placement are 6 8mm machined holes used to bolt the BGM in place. A second loose annulus with identical dimensions is mounted on top of the BGM to secure it in place (Rogal et al., 2021).

Figure 2: Puncturing probe next to side profile of mount

## 2.6 ASTM Tear Assembly

The equipment used to perform the tear testing uses the same pneumatic cylinder frame as the puncture apparatus. There are two custom clamping grips that attach to the top and bottom of the cylinder assembly frame. The top clamp remains static, while the lower clamp can raise and lower with the stroke of the cylinder. The clamps in the load frame can be seen in Figure 3.

Figure 3. Tearing Clamps in Pneumatic Cylinder

## 2.7 Testing Preparation

In preparation for the tests, the samples were cut to the proper size for the respective tests (puncture, tear, performance) and then left to equilibrate inside the main temperature control units for 24 hours at the test temperature.

The temperature was controlled during testing using walk-in climate chambers for the above-zero tests, and a commercial walk-in freezer unit for the sub-zero tests in the facility at the U of S. The units are large enough for the testing apparatus to be set up inside, allowing for the entire setup to be at the desired temperature. Both the climate chamber and freezer unit were given 24 hours to equilibrate and reach the desired temperature before testing began. There were also multiple thermometers in place to ensure the correct temperature was reached, both integrated into the climate chamber unit, and mounted inside the chamber independently (Rogal et al., 2021).

## 2.6 Large Scale Apparatus

The large-scale test apparatus uses the same pneumatic cylinder frame to apply and maintain load, however the apparatus that the experiment is contained in is a custom fabricated load assembly. The assembly consists of three main steel fabricated pieces, as well as connections for various equipment.

The three main pieces are the lower body cylinder, the upper body cylinder, and the load cap plate. The two body cylinders are stacked on top of each other over an o-ring seal and clamped together using six threaded rods. The body contains the subgrade, the barrier material being tested, and the overburden aggregate. The load plate is a shallow, hollow cylinder with an NPT fitting on top, and three o-ring grooves along the outer wall to seal to the inside of the main body. Water can be pumped into the plate from the top of the hollow body, and then flow freely out through the drainage holes in the bottom of the plate to enter the system. The apparatus can be seen in figure 4.

Figure 4: Large Scale Load Apparatus

To monitor the load for the apparatus, a round ball bearing fitting is set between the assembly and the load cell, which can then log the load applied to the system from the air cylinders. A GDS Labs Pressure/Volume controller is used to apply and monitor the hydraulic head in the system via the NPT fitting on top of the load plate. The air flow is controlled using the equipment described in Section 2.4

# 3.0 RESULTS & DISCUSSION

## 3.1 BGM Puncture Results

### 3.1.1 ES2 Results & Discussion

The peak resistance and displacement values at each temperature increment were recorded along with plots showing the average response of the ES2 samples shown in Figure 5. It is worth noting that for Figure 5 and Figure 6, noise in the data post-rupture is caused by allowing data to be logged for slightly different durations after puncture has been produced and does not impact the force required for puncture. Based on Figure 5, there was no major difference between the response of the material at most positive temperatures. However, at 30°C the average puncture resistance of the material was significantly lower at around 230 N, while the rest of the trials sat around 370 N puncture resistance. Though the required force to puncture the BGM was significantly lower at 30°C, the displacement required to initiate that puncture was still similar (Rogal et al., 2021).

The highest puncture resistance occurred at -20°C, with a resistance of around 590 N. The data presented in Table 5 shows the peak responses of the ES2 samples at each temperature. Like the average responses at each temperature, 0-20°C have similar peak response values in puncture resistance, with the 30°C response being slightly lower. When it comes to peak displacement responses for the ES2 samples, the 0-10°C trials all showed similar peak displacement values at puncture of around 25 mm, while the 20-30°C reached peak displacements of around 34 mm. The sub-zero temperatures showed much lower peak displacements at around 10mm (Rogal et al., 2021).

Table 5. Peak Values of ES2 Puncture Testing

| Temperature (°C) | Puncture Res. (N) | Displacement (mm) |
|---|---|---|
| -20 | 590.29 | 9.27 |
| -10 | 555.17 | 11.96 |
| 0 | 426.65 | 24.67 |
| 5 | 425.63 | 25.61 |
| 10 | 392.06 | 25.43 |
| 20 | 468.80 | 34.52 |
| **30** | 337.35 | 33.34 |

### 3.1.2 ES4 Results and Discussion

Like the ES2 tests, 3 to 4 tests were conducted on the ES4 product at each temperature. The average and peak

puncture resistance, and displacements were recorded at each temperature and subsequently analyzed (Rogal et al., 2021). Figure 6 shows the plot of average response of puncture resistance versus displacement (the post-rupture noise in the data is like that of Figure 5).

The data shown in Figure 6 follows similar trends to that of the ES2 responses, however the trend it slightly more noticeable than that of the ES2.

The 0-10°C tests all show higher resistance to puncture, and lower amounts of displacement before puncture occurs. For those three test temperatures the average puncture resistance is estimated to be around 550-650 N, with an average displacement of 25mm before rupture occurs. This trend continues as the temperatures reach -10°C and -20°C when the average puncture resistance increases even further to 966.9 N and 1194.8 N respectively. The average displacement required for puncture also decreased substantially for the -10°C and -20°C tests to 13.2 mm and 9.8 mm respectively.

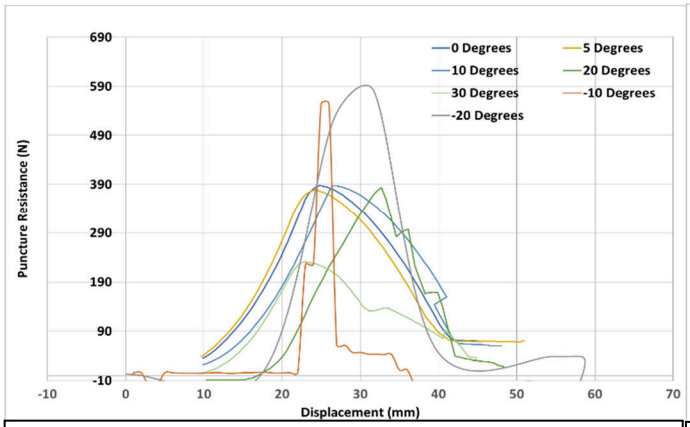


Figure 5: ES2 Average Responses of Puncture Resistance Vs Displacement with Variation in Temperature

For the warmer test temperatures (20-30°C) the average puncture resistance is noticeably lower at 400-450 N, both with average displacements of roughly 35 mm before rupture. The peak responses of the ES4 product in each temperature trial are presented in Table 6, and again show similar trends to that of Table 5 and the ES2 product.

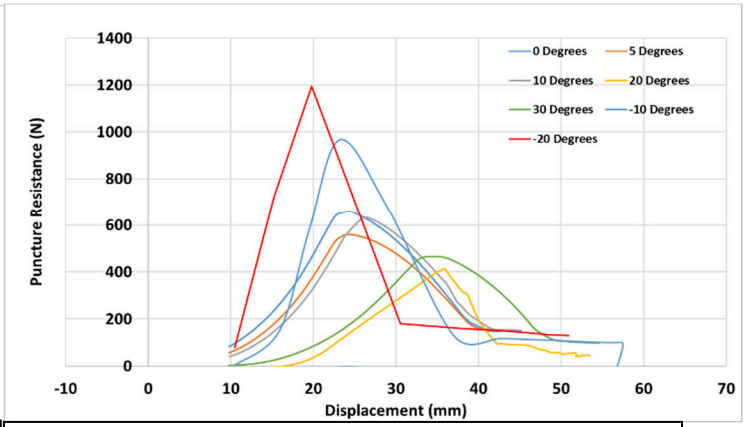


Figure 6: ES4 Average Responses of Puncture Resistance Vs Displacement with Variation in Temperature

Table 6. Peak Values of ES4 Puncture Testing

| Temperature (°C) | Puncture Res. (N) | Displacement (mm) |
|---|---|---|
| -20 | 1194.76 | 9.75 |
| -10 | 966.88 | 13.17 |
| 0 | 731.67 | 23.97 |
| 5 | 600.87 | 24.28 |
| 10 | 678.50 | 24.47 |
| 20 | 454.15 | 36.38 |
| 30 | 498.49 | 33.32 |

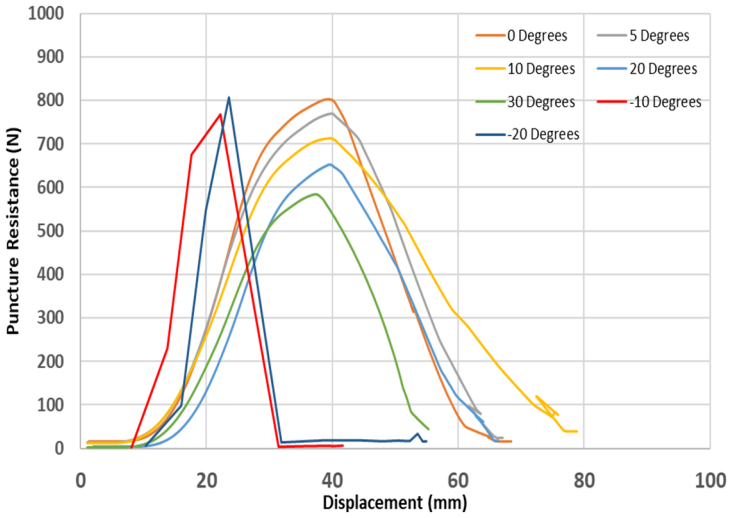


Figure 7: 1.5 mm HDPE Average Responses of Puncture Resistance Vs Displacement w/ Temperature Variation

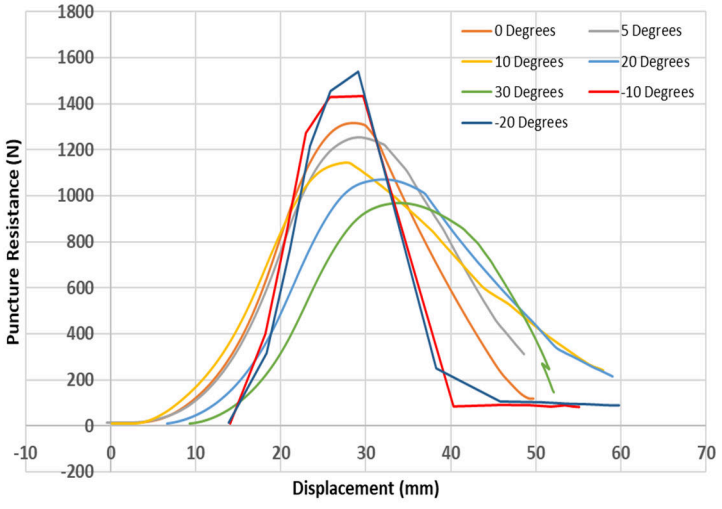


Figure 8. 3 mm HDPE Average Responses of Puncture Resistance Vs Displacement w/ Temperature Variation

### 3.2 HDPE Puncture Results

The Solmax High Density Polyethylene geomembranes followed similar trends to that of the ES BGM products, and the tests were conducted under the same preparations and conditions. The samples were cut to 11 cm x 11 cm sample size and let to equilibrate in the temperature-controlled environments for 24 hours prior to the testing being completed.

The results for the 1.5 mm HDPE (seen in figure 7) show very slight change in required force for puncture across all temperatures, as well as displacement achieved at the time of puncture. The most significant variation was that the sub-zero tests showed a much more noticeable decrease in displacement for puncture, which is expected as the rigidity of the HDPE would increase at lower temperatures. The range of puncture and displacement values for the 1.5 mm HDPE were found to be 590 N to 807 N, and 37 mm to 13 mm from higher to lower temperatures respectively.

In the 3 mm HDPE testing, there were more noticeable changes in the puncture resistance of the samples, and similar displacement trends to that of the 1.5 mm HDPE which is expected. The range of puncture and displacement values for the 3 mm HDPE were found to be 990 N to 1540 N, and 33 mm to 15 mm from higher to lower temperatures respectively. The results can be seen in figure 8. The compiled results of the HDPE puncture tests can be seen in the tables 7 and 8.

Table 7. Peak Values of 1.5 mm HDPE Puncture Testing

| Temperature (°C) | Puncture Res. (N) | Displacement (mm) |
|---|---|---|
| -20 | 807.0 | 13.2 |
| -10 | 767.7 | 14.1 |
| 0 | 809.1 | 39.6 |
| 5 | 809.4 | 41.0 |
| 10 | 724.5 | 42.5 |
| 20 | 675.0 | 40.5 |
| 30 | 590.0 | 37.8 |

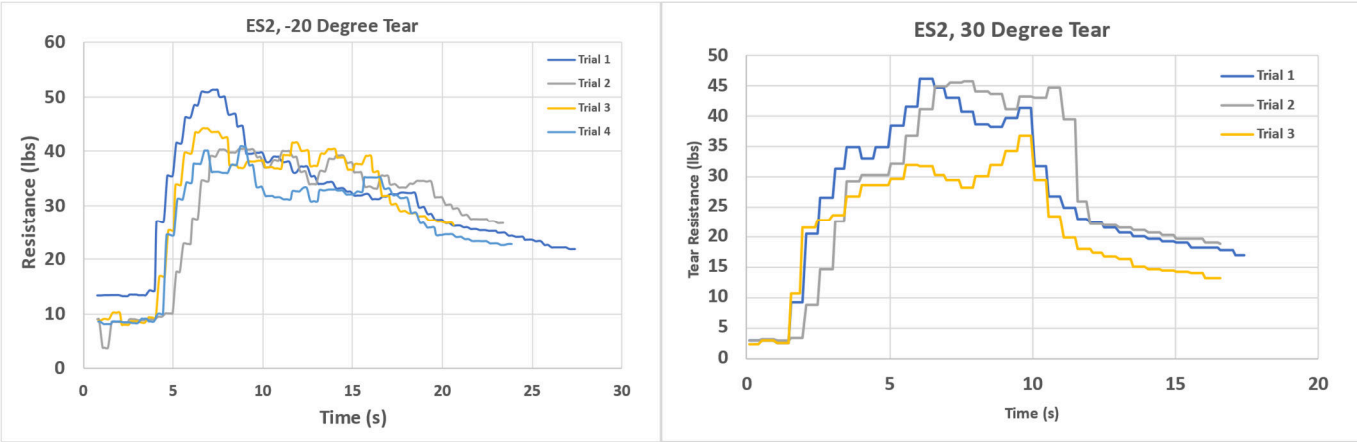


Figure 9: ES2 Tear Results

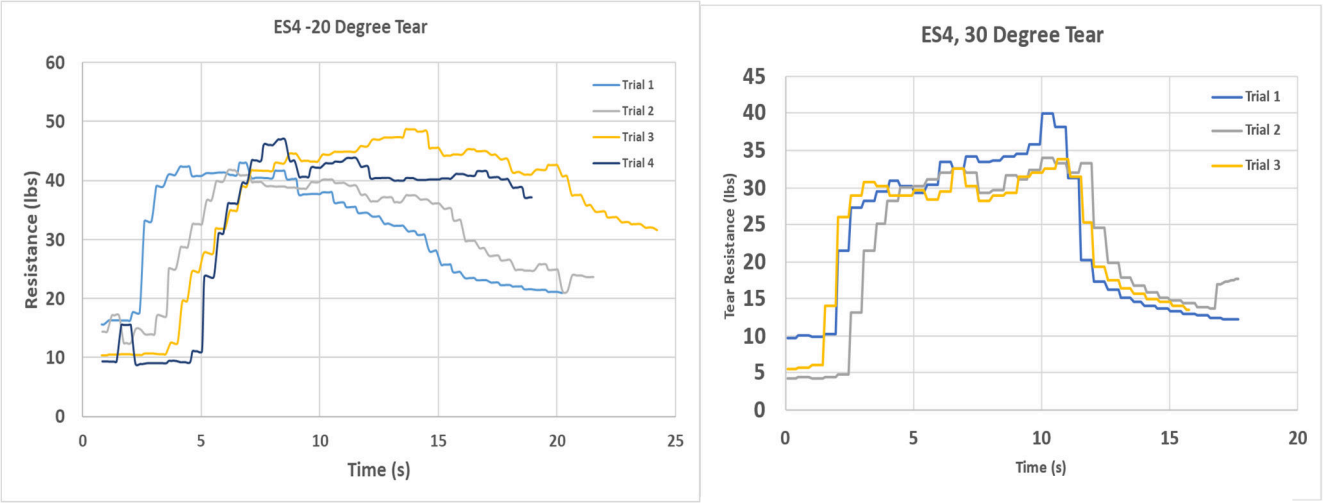


Figure 10: ES4 Tear Results

Table 8. Peak Values of 3 mm HDPE Puncture Testing

| Temperature (°C) | Puncture Res. (N) | Displacement (mm) |
|---|---|---|
| -20 | 1540.9 | 15.2 |
| -10 | 1432.1 | 15.6 |
| 0 | 1338.7 | 28.5 |
| 5 | 1320.2 | 28.4 |
| 10 | 1192.4 | 28.0 |
| 20 | 1091.4 | 31.5 |
| 30 | 998.6 | 33.9 |

### 3.3 Trends in Puncture Peak Values

When observing the results of the puncture versus displacement graphs, it is worth noting that the displacements recorded are from when contact is made between the puncture probe and the sample (when an increase in resistance is first recorded) and the peak puncture value. The x-axis scale simply records the overall movement of the probe from test start, which is not in contact with the sample for the entire time. In general, the peak responses follow similar trends between the ES2 and ES4 products, as well as the HDPE products. All four samples exhibit higher resistance to puncture at lower temperatures, and larger displacements before puncture at higher temperatures. When looking at peak puncture resistance versus temperature, the ES2 sample did not show as much variation as the ES4 samples (Rogal et al., 2021). The ES2 sample peaks were much less scattered than that of the ES4 samples. The peak displacement did tend to increase with temperature in both products by nearly 30% from the low to high end. Overall, both sets of products (ES line and HDPE) showed a positive correlation between temperature and displacement, and a negative correlation between temperature and puncture resistance.

### 3.4 Tear Results

The tear result section will include comparisons between the highest and lowest temperature values for the selected ES samples, as to show the little variation in the numerical results. Most of the variation was in the way in which the samples tore, not the resistance values themselves. The results are shown in figures 9 and 10.

There was very little difference in the tear resistance of the ES2 and ES4 materials with a variation in temperature. The peak tear resistances at -20°C and 30°C were both within the 40-50 lb range, except for the ES4 being in the 30-40 lb range, which can be seen in figures 9 and 10. The main difference between the two temperature increments were the post-peak reactions. At -20°C, the samples reached their peak tear resistance values after only a few seconds which then slowly decreased as the tearing continued. At 30°C, there was a more gradual increase to the peak tear resistance, which then remained near constant for the remainder of the test after it was achieved.

### 3.5 Large Scale Observations/Results

Currently, only a handful of large-scale apparatus tests have been completed on the ES2 and ES4 products. The tests lasted 5 days from start to finish under maximum stresses of around 0.8 – 1 MPa. All the tests completed have been done at 20°C and the applied head from the GDS Labs PV controller was set to maintain a constant 10 kPa. In addition to coarse aggregate, multiple larger, more aggressive pieces of aggregate were also placed directly on top of the BGM surface to try and force as much potential puncture as possible, however in all the completed tests no puncture was experienced. There was considerable damage to the BGMs in the form of

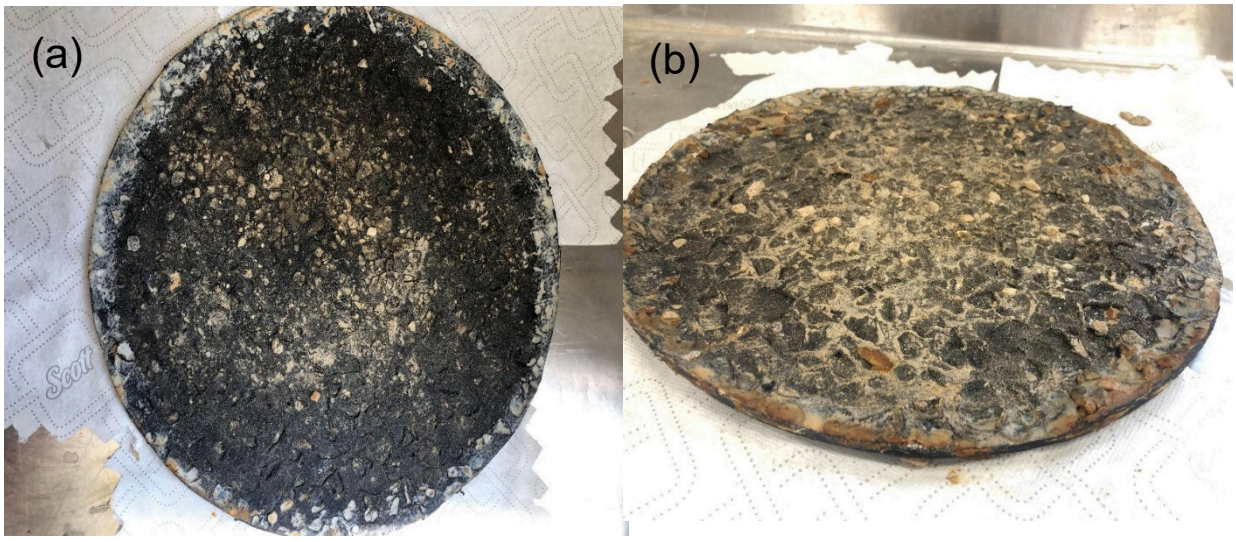


Figure 11: Top view of ES4 after performance test (a) and side profile of ES2 after performance test

indentations and deformation, however none of the imprints fully punctured the samples. This was verified by holding the sample up to a bright light to see if any light was visible through the BGM. There were also no noticeable changes on the recorded head from the PV controller, further signifying there were no holes present that the machine would then need to account for.

Additionally, the 'self healing' effect that has been proposed by Clinton and Rowe (2017) was very apparent during these tests. There were many smaller pieces of aggregate lodged in place in the BGM where they had been present, with the material itself moulding around them. Figure 11 a) and b) show some of the clear indentation and damage that was sustained by the BGM during these large-scale tests.

## 4.0 CONCLUSION

When evaluating the results of these tests, and by visual analysis during the test, it was observed that in warmer test environments the samples had a much more ductile response to the puncture test with a nearly 30% increase in displacement over the lower temperature tests. Similarly, the materials responded in a more brittle manner when tested at lower temperatures. Higher forces were required for puncture at low temperatures, especially in the case of ES4. When looking at the results of the tear tests, there was no significant change in tear resistance between temperature ranges, however there was a noticeable change in the post-peak response to how the material tore. Lower temperatures showed a gradual decrease in resistance after the peak was reached, whereas in the warmer temperatures the peak resistance was help consistently until the end of the test.

For all material types tested, there were clear correlations between the temperature at which they were being tested, and the values recorded from the testing. An increase in temperature leads to more deformation/displacement in the sample, as well as lower peak resistance to puncture, while a decrease in temperature leads to higher resistance but lower displacement needed to reach that puncture. It can still be confidently stated that HDPE retains a higher resistance to puncture than BGMs, however the ductile nature of BGMs shows that it could have many advantages depending on the conditions in which it is used

## 5.0 FUTURE WORK

The remaining work for this project includes more large-scale apparatus testing of BGMs in a variety of temperature-controlled settings and evaluating the results of these tests. The results of these temperature increments will also be evaluated against each other to evaluate how the materials perform under these conditions, and additionally compared to that of similar HDPE products.

## 6.0 ACKNOWLEDGEMENTS

The authors thank NSERC and University of Saskatchewan for financial support for this project. The authors are also grateful to their industrial partner, Titan Environmental Containment Ltd., for supplying Coletanche -BGM's and providing technical and financial support for this project.

## 7.0 REFERENCES

ASTM FOR BGM, and ASTM. 2012. Standard Test Method for Tensile Properties of Bituminous Geomembranes ( BGM ). Astm, **i**(C): 7–8. doi:10.1520/D7275-07R18.2.

ASTM International. 2010. Standard Test Method for Index Puncture Resistance of Geomembranes and Related. (C): 8–11. doi:10.1520/D4833-07.2.

Axter Colentache® Inc. 2009a. ES2 Product Data Sheet. Packaging (Boston, Mass.),: 10–11.

Axter Colentache® Inc. 2009b. ES4 Product Data Sheet. Packaging (Boston, Mass.),: 10–11.

Axter Colentache® Inc. 2020. Range of Products. Available from http://www.coletanche.com/en/geomembrane/gamme.

Clinton, M., and Rowe, R.K. 2017. Physical Performance of a Bituminous Geomembrane for use as a Basal Liner in Heap Leach Pads.

Lambert, S., and Touze, N., 2000. A test for measuring permeability of geomembranes mumolade View project A test for measuring permeability of geomembranes.

Rogal, M., Fleming, I., Marcotte, B., Bhat, S. 2021. Short Term Durability and Performance of Bituminous Geomembranes with Respect to Temperature. GeoNiagara 2021 Conference Proceedings

Touze-Foltz, N., and Farcas, F. 2017. Long-term performance and binder chemical structure evolution of elastomeric bituminous geomembranes. Geotextiles and Geomembranes,. doi:10.1016/j.geotexmem.2017.01.003.

Touze-foltz, N., Farcas, F., and Benchet, R. 2015. Evaluation of the Ageing of Two Bituminous Geomembranes of Different Natures After 15 Years in Service. **10318**: 142–151.